Design and optimization of one-dimensional photonic crystals for thermophotovoltaic applications

Ivan Celanovic, Francis O'Sullivan, Milos Ilak, John Kassakian, and David Perreault

Massachusetts Institute of Technology, 77 Massachusetts Avenue, Cambridge, Massachusetts 02139

Received October 3, 2003

We explore the optical characteristics and fundamental limitations of one-dimensional (1D) photonic crystal (PhC) structures as means for improving the efficiency and power density of thermophotovoltaic (TPV) and microthermophotovoltaic (MTPV) devices. We analyze the optical performance of 1D PhCs with respect to photovoltaic diode efficiency and power density. Furthermore, we present an optimized dielectric stack design that exhibits a significantly wider stop band and yields better TPV system efficiency than a simple quarter-wave stack. The analysis is done for both TPV and MTPV devices by use of a unified modeling framework. © 2004 Optical Society of America

OCIS codes: 230.2090, 230.4170, 310.0310, 350.2460.

Thermophotovoltaics (TPVs) are static energy converters that convert thermal radiation into electricity by means of a photovoltaic (PV) diode. The TPV device consists of an emitter, a PV diode, and a spectral control component (filter). The emitter converts heat into radiation (mostly in the near infrared), which is selectively filtered by an optical filter. Part of the radiation is transmitted, and the rest is reflected back to the emitter. The PV diode converts the transmitted photons with energies in excess of the diode bandgap energy into charge carriers, whereas the photons below the bandgap energy are partially absorbed, converted into waste heat, and partially reflected back to the emitter by the back-side contact. In this Letter we investigate the performance of one-dimensional (1D) photonic crystals (PhCs), such as dielectric stack structures, as front-side filters for TPV applications, explore their design limitations, and present an optimized dielectric stack design.

We analyze the TPV system that consists of an emitter, a gap between the emitter and the diode, a 1D PhC, and a PV diode, as shown in Fig. 1. The performance of the TPV system is assessed with respect to the efficiency and power density delivered by the diode.

The amount of power radiated from the blackbody source at temperature T_{BB} to the PV diode can be calculated using an ideal thermodynamic model[1,2]:

$$P_{\mathrm{rad}} = \int_0^{\infty}\int_0^{\theta_1} \cos\theta \sin\theta \frac{\hbar\omega}{\exp(\hbar\omega/kT_{\mathrm{BB}})-1} \times \frac{n_{\mathrm{BB}}^2\omega^2}{(2\pi)^2c^2}\mathrm{Tr}_{13}(\omega,\theta)\mathrm{d}\theta\mathrm{d}\omega - \int_0^{\infty}\int_0^{\theta_3} \cos\theta \sin\theta \frac{\hbar\omega}{\exp[(\hbar\omega-\mathrm{eV})/kT_{\mathrm{PV}}]-1} \times \frac{n_{\mathrm{PV}}^2\omega^2}{(2\pi)^2c^2}\mathrm{Tr}_{31}(\omega,\theta)\mathrm{d}\theta\mathrm{d}\omega\,, \quad (1)$$

where T_{PV} is the diode temperature; n_{BB} and n_{PV} are the blackbody and diode refractive indices, respectively; $\theta_1 = \arcsin(n_{\mathrm{PV}}/n_{\mathrm{BB}})$ for $n_{\mathrm{PV}} < n_{\mathrm{BB}}$ and $\theta_1 = \pi/2$ otherwise; and $\theta_3 = \arcsin(n_{\mathrm{BB}}/n_{\mathrm{PV}})$ for $n_{\mathrm{PV}} > n_{\mathrm{BB}}$ and $\theta_3 = \pi/2$ otherwise. The first term in Eq. (1) is the total power transferred from the blackbody to the PV diode (integrated over all frequencies and all angles of incidence), whereas the second term is the amount of power reradiated back to the emitter by the diode. Tr_{13} is the sum of the TE and TM mode transmittances from the emitter to the diode, which is function of the frequency ω, the angle of incidence θ (as shown in Fig. 1), and the gap length L_o. Tr_{31} is the transmittance from the diode to the emitter. The electrical power per unit area generated by the diode is calculated as the product of the resultant photon flux (power divided by photon energy $\hbar\omega$, assuming a quantum efficiency of 1), the electron charge e, and the applied voltage V:

$$P_{\mathrm{PV}} = eV\left\{\int_{\omega_g}^{\infty}\int_0^{\theta_1} \cos\theta \sin\theta \frac{1}{\exp(\hbar\omega/kT_{\mathrm{BB}})-1} \times \frac{n_{\mathrm{BB}}^2\omega^2}{(2\pi)^2c^2}\mathrm{Tr}_{13}(\omega,\theta)\mathrm{d}\theta\mathrm{d}\omega - \int_{\omega_g}^{\infty}\int_0^{\theta_3} \cos\theta \sin\theta \frac{1}{\exp[(\hbar\omega-\mathrm{eV})/kT_{\mathrm{PV}}]-1} \times \frac{n_{\mathrm{PV}}^2\omega^2}{(2\pi)^2c^2}\mathrm{Tr}_{31}(\omega,\theta)\mathrm{d}\theta\mathrm{d}\omega\right\}, \quad (2)$$

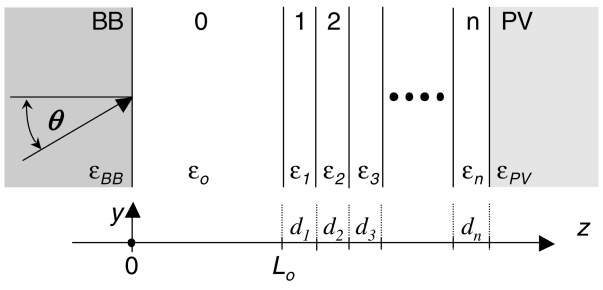

Fig. 1. TPV system with a front-side dielectric stack filter (layers 1–n), in which the thickness of the gap (layer 0) between the emitter (BB) and the dielectric stack is L_o. The PV diode extends to $+\infty$.

0146-9592/04/080863-03$15.00/0

where ω_g is the diode bandgap frequency. By use of Eqs. (1) and (2), efficiency is defined as

$$\eta_{\mathrm{TPV}} = \frac{P_{\mathrm{PV}}}{P_{\mathrm{rad}}}. \tag{3}$$

It is apparent from Eqs. (1)–(3) that by tailoring Tr_{13} one can dramatically influence the performance of the TPV system. For example, unlike for small L_o, for large L_o the transmittance does not depend on the gap size. For small L_o the large number of modes that are evanescent in the gap couple into the diode, thus increasing the overall power transfer.[2] In this case Tr_{13} is largely dependent on L_o. In the large gap case none of the evanescent modes can tunnel through the gap; therefore power is transferred through propagating modes only. The system architecture is the same in both cases, but the power transfer regimes are qualitatively different. Ideally, a PhC filter deposited on the surface of the diode should strongly couple all the electromagnetic radiation modes above the bandgap ($\mathrm{Tr}_{13} = 1$ for $\omega > \omega_{\mathrm{gap}}$) and not couple the low frequency modes ($\mathrm{Tr}_{13} = 0$ for $\omega < \omega_{\mathrm{gap}}$). To understand the nature of this selective coupling of external radiation, we analyze the photonic band structure of PhCs, which provides us with insight about the transmittance and reflectance of the structure.

The projected photonic band diagram of an infinite 1D PhC composed of alternating layers of Si and SiO_2, shown in Fig. 2, is calculated using the analytical solution as in Ref. 3. The propagating modes are shaded, and the white areas represent nonpropagating modes. Although a 1D PhC does not exhibit a full bandgap, when coupled to free space, it can exhibit total omnidirectional reflectance.[4] The condition for omnidirectional reflection is that there is no overlap between projected PhC bands and projected ambient structure bands for certain ranges of frequencies. The projected band structure for free space is the cone above the light line characterized by $\omega_2 = 1/(\mu\varepsilon)(k_y^2 + k_z^2)$, which is filled with allowed modes.

In the large gap limit ($L_o \to \infty$)—the standard TPV case—the PhC exhibits omnidirectional reflection. In the small gap limit ($L_o \to 0$)—the microthermophotovoltaic (MTPV) case—the emitter light line has a slope of $(\varepsilon_{\mathrm{BB}})^{1/2}$ that is usually larger than 1 (where $\varepsilon_{\mathrm{BB}} = 6.7$ for the SiC emitter and $\varepsilon_{\mathrm{PV}} = 14.5$ for the GaSb diode). When the PhC is closely coupled to the emitter with a refractive index of $n_{\mathrm{BB}} > 1$, the total reflection band vanishes since the emitter light lines do not intersect the projected bandgap, as shown in Fig. 2. Although one can obtain omnidirectional reflection for a large gap, for a small gap it is difficult.

To quantify the performance limits of a PhC applied to a TPV, we calculate the transmittance of two finite ten-layer dielectric stacks of $Si-SiO_2$ deposited on a PV diode. The first design is the modified quarter-wave stack (MQWS). The difference between the quarter-wave stack and the MQWS is that the former has a $LHLHL \ldots HLHL$ refractive-index profile, whereas the latter has a $(L/2)HLHLHLHL(H/2)$ profile. The addition of half-layers at the front and back reduces the ripple in the passband, which helps preserve the power density of the system. Normal-incidence transmittance for the MQWS is shown in Fig. 3. A large normal-incidence stop band can be observed from 1.8 to 3.2 μm, which directly corresponds to the one observed in the projected band diagram in Fig. 2 (ω_n exhibits a normal-incidence bandgap from 0.175 to 0.31, where $\lambda = a/\omega_n$ and $a = 0.56$ μm is the period of the 1D PhC). The cutoff wavelength is 1.8 μm and corresponds to the electron bandgap of GaSb. The layer thicknesses are given in Table 1.

The second design—a genetic-algorithm optimized stack (GAOS)—was developed using a real-valued genetic-algorithm-based optimization routine.[5] The optimization problem was formulated to search for a dielectric stack structure that maximizes the cost function defined as the weighted sum of the diode efficiency [as defined in Eq. (3)] and (or) the power density [Eq. (2)]. The constraint was the number of layers and materials used, while the independent variables were individual layer thicknesses. The transmittance of the optimal design that maximizes the efficiency is shown in Fig. 3(b). This design

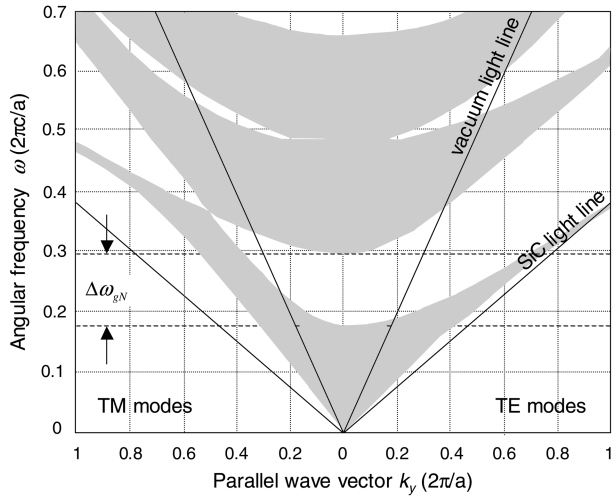

Fig. 2. Projected photonic band diagram for a 1D $Si-SiO_2$ quarter-wave stack for both polarizations (TE and TM). Light lines represent $\omega = 1/(\mu\varepsilon)^{1/2}k_y$ for both vacuum ($\varepsilon = \varepsilon_0$) and SiC ($\varepsilon = 6.7\varepsilon_0$). Normal-incidence bandgap is designated as $\Delta\omega_{gN}$.

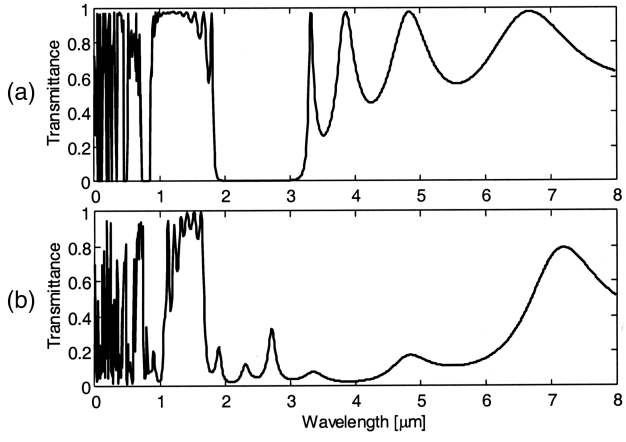

Fig. 3. Transmittance at normal incidence for (a) MQWS and (b) GAOS. Layer thicknesses are given in Table 1.

Table 1. Dielectric Stack Layer Thicknesses (μm)

Stack	d_1	d_2	d_3	d_4	d_5	d_6	d_7	d_8	d_9	d_{10}
MQWS	0.195	0.17	0.39	0.17	0.39	0.17	0.39	0.17	0.39	0.085
GAOS	0.164	0.396	0.894	0.183	0.894	0.2	0.48	0.191	0.436	0.003

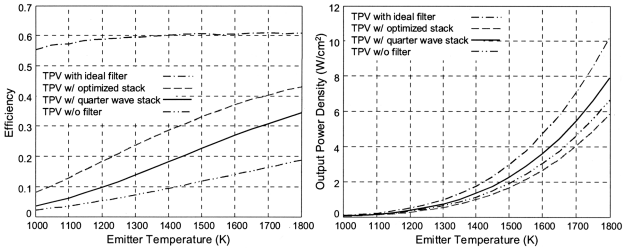

Fig. 4. Efficiency and power density versus the emitter temperature for a GaSb standard TPV system with an ideal cutoff filter, MQWS, GAOS, and without a filter.

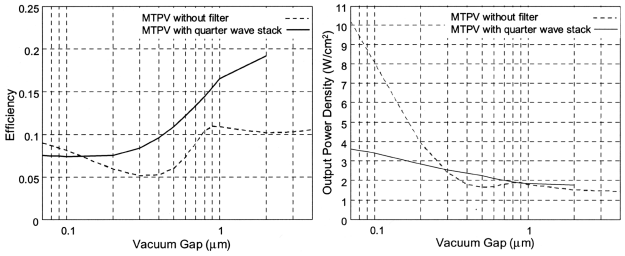

Fig. 5. Efficiency and power density versus vacuum gap for a GaSb MTPV system without filter and with MQWS for an emitter temperature of 1500 K.

exhibits a much wider stop band at some cost to the passband region. The layer thicknesses are given in Table 1. Our experience in manufacturing $Si-SiO_2$ stacks shows that, because of a large index contrast, these designs are robust to layer thickness variation, but we will address this issue in a subsequent publication. Efficiency and power density versus emitter temperature for TPV systems with MQWS, GAOS, an ideal high-pass filter, and without a filter—calculated using Eqs. (1)–(3), thus taking into account the angular dependence of the transmittance—are shown in Fig. 4. The TPV system with an optimized stack shows almost 10% better efficiency than one with a MQWS over the range of temperatures. The MQWS has better output power density because of its wider passband and lower ripple. By changing the cost function in our optimization routine, we can sweep the entire efficiency–power density design space.

In the MTPV case—in which the gap is smaller than the wavelength of radiation—the power transfer regime is different from the TPV. The evanescent modes in the gap coupled to the dielectric stack, and, since they have large k_y vectors, it is difficult to filter them out. Also, note in Fig. 2 the absence of total omnidirectional reflectance as well as the absence of strong coupling of all high-frequency modes. Figure 5 shows the output power density and efficiency versus the gap length for the MTPV system—calculated using Eqs. (1)–(3)—without any filter and with a MQWS. The MTPV system with a quarter-wave stack is more efficient than the unfiltered MTPV for gaps greater than 0.1 μm. Below 0.3 μm the unfiltered MTPV exhibits better power density since it exhibits stronger coupling to high-frequency modes than the MTPV with a PhC filter, largely due to bandgap curvature.

In conclusion, we have analyzed TPV devices with 1D PhC optical components by use of an ideal thermodynamic model for a blackbody emitter. We have presented a unified treatment of a TPV system applicable to both the TPV and the MTPV. We have studied the modified quarter-wave stack performance as a front-side filter for both types of TPV and proposed the optimized filter design that exhibits a significant improvement in efficiency with slightly reduced power density, with the same number of layers as MQWS. For the MTPV the system with a dielectric stack filter has better efficiency than the unfiltered one for gap lengths greater than 0.1 μm and better power density above 0.3 μm. The unanswered question remains—how can one simultaneously filter radiation and achieve good coupling for MTPV devices with a small gap?

The authors thank Robert DiMatteo and Marc Weinberg of Draper Laboratories, Inc. for numerous discussions and valuable suggestions. This work was sponsored by the Massachusetts Institute of Technology Industry Consortium on Advanced Automotive Electrical/Electronic Components and Systems.
I. Celanovic's e-mail address is ivanc@mit.edu.

References

1. M. Zenker, A. Heinzel, G. Stollwerck, J. Ferber, and J. Luther, IEEE Trans. Electron. Devices **48,** 367 (2001).
2. J. L. Pan, H. K. H. Choy, and C. G. Fonstad, IEEE Trans. Electron. Devices **47,** 241 (2000).
3. P. Yeh, *Optical Waves in Layered Media* (Wiley, New York, 1988), pp. 118–123.
4. J. N. Winn, Y. Fink, S. Fan, and J. D. Joannopoulos, Opt. Lett. **23,** 1573 (1998).
5. C. Houck, J. Joines, and M. Kay, "A Genetic Algorithm for Function Optimization: a Matlab Implemenation," Tech. Rep. NCSU-IE Tr 95-09 (North Carolina State University, Raleigh, N.C., 1995).